Atomic Resolution of Structural Changes in Elastic Crystals

Anna Worthy,[1*] Arnaud Grosjean,[2*] Michael C. Pfrunder,[2] Yanan Xu,[1] Cheng Yan,[1] Grant Edwards,[3] Jack K. Clegg[2] and John C. McMurtrie[1]

[1] School of Chemistry, Physics and Mechanical Engineering, Faculty of Science and Engineering, Queensland University of Technology (QUT), GPO Box 2434, Brisbane, QLD, 4001

[2] School of Chemistry and Molecular Biosciences, The University of Queensland, St Lucia, QLD, 4072, Australia

[3] Australian Institute of Bioengineering and Nanotechnology, The University of Queensland, St Lucia, QLD, 4072, Australia

*These authors contributed equally to this work.

Crystalline materials are thought of as brittle, inelastic materials. Such mechanical responses limit the use of these materials in new applications like flexible electronics and optical devices. However, we have discovered single-crystals of a metal-organic material that are flexible enough to be reversibly tied into a knot. Mechanical measurements of these crystals indicate that they have elasticity similar to soft materials like nylon, thus displaying properties normally associated with both hard and soft matter. Using micro-focused synchrotron radiation we have mapped the changes in crystal structure that occur with bending and determined the mechanism that allows this flexibility with atomic precision. We show that with the application of strain the molecules in the crystal reversibly rotate, thus reorganising to allow the induced mechanical compression and expansion required for elasticity while maintaining the integrity of the crystal structure.

Crystallinity, a property of hard matter, underpins a wide variety of existing modern technologies including semi-conductors and lasers.[1-4] The regular arrangement of molecules in crystal lattices is required for new high-strength industrial components and the development of emerging gas adsorption and sequestration technologies.[5-8] Crystalline materials, however, are commonly hard and brittle, when they are struck or bent they typically crack, shatter or deform irreversibly.[1,9-12] Such mechanical responses limit the use of these materials in new applications like flexible electronics and optical devices.[2] Crystals that could be reversibly and repeatedly bent, characteristics normally associated with soft matter, would be extremely attractive for use in myriad engineering applications that require materials in which properties can be tuned through external stimuli.[5,13-16]

Recently there have been several reports of organic molecular crystals that exhibit plastic (irreversible) bending.[1,9-12] Here we describe single crystals of a metal-organic material that display significant elastic flexibility. Acicular crystals of *bis*(acetylacetonato)copper(II) ([Cu(acac)$_2$]) (Fig. 1a), a classical coordination compound,[17] are so flexible they can be repeatedly and reversibly twisted and bent without losing crystallinity (Supplementary Video 1). They can even be tied into a knot (Fig.1b). Through synchrotron X-ray measurements we have mapped the changes in crystal structure that occur when these crystals are bent and determined the mechanism that allows elastic flexibility with atomic resolution.

Results and Discussion

The crystal structure of [Cu(acac)$_2$] (Fig. 1c), was first reported in 1969[18] and is isomorphous (monoclinic, $P2_1/n$) between 100 K - 298 K (CSD Ref Codes: ACACCU and ACACCU01-05).[19-23] The

[Cu(acac)$_2$] molecules are planar and stack closely together along the crystallographic *b* axis. The mean planes of the molecules within each stack are exactly parallel and inclined with a dihedral angle of 48.7 ° from the (010) plane. This supramolecular stacking is facilitated by π-π interactions of delocalised electronic systems[24,25] and by relatively strong Cu-π interactions.[26] The dominant supramolecular connectivity (π-π and Cu-π) is one-dimensional with only weak dispersive interactions propagating in other directions. Face-indexing confirmed the relationship between the crystal packing and the crystal morphology. The crystal faces coincide with the crystallographic (101) and (10$\bar{1}$) planes as shown in Figure 1c. The longest metric dimension of the crystals coincides with the crystallographic *b* axis (i.e. [010]). These crystals can be repeatedly bent along the [010] direction and the (101) and (10$\bar{1}$) faces (which are not equivalent under the symmetry of the monoclinic space group $P2_1/n$). Removal of the force bending the crystals results in the crystals quickly returning to their original shape with no signs of breaking or cracking (Supplementary Video 1). Single crystal X-ray diffraction experiments both before and after bending showed no loss of crystallinity (Supplementary Table 7). While bent however, Bragg peaks in the diffraction pattern were broadened (Fig. 3a), which indicates loss of long range order due to differences in molecular separations induced by bending.

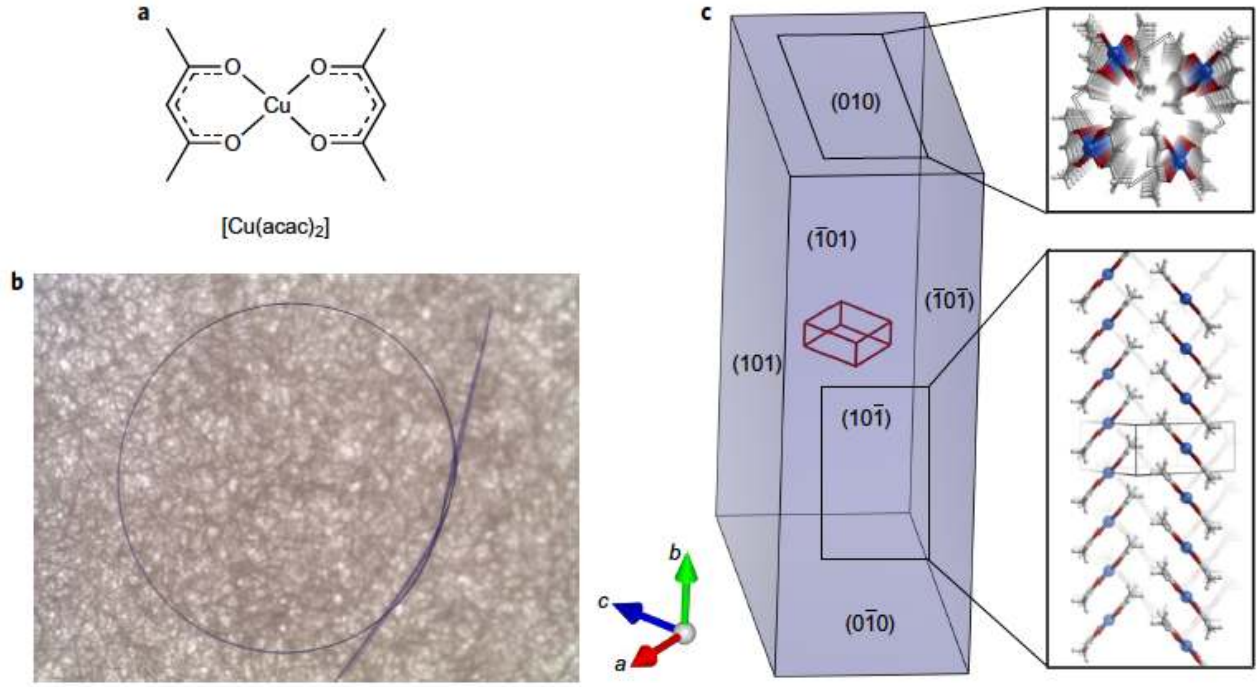

Figure 1 Crystal Structure of [Cu(acac)$_2$]. a, Chemical structure of [Cu(acac)$_2$]. **b**, A [Cu(acac)$_2$] crystal tied (reversibly) in an overhand knot. **c**, Two views of the crystal structure of unbent [Cu(acac)$_2$] viewed along the [010] and [10$\bar{1}$] directions as determined by face indexing.

Mechanical Characterisation

The flexibility of the crystals was characterised with a suite of mechanical techniques. The surface hardness and elastic moduli of the [Cu(acac)$_2$] crystals were measured using nano-indentation (Figs. 2a and 2d). The hardness of the (101) face was found to be in the range 200-240 MPa with an elastic modulus between 4.8-6.9 GPa. The hardness of the (10$\bar{1}$) face was 380-400 MPa and the elastic modulus 11.3-13.8 GPa, significantly larger than the (101) face. These values are typical of molecular materials and metal organic frameworks.[27]

We then measured the tensile elasticity of the crystals by stretching four individual single crystals (Figs. 2b and 2e). The crystals could be stretched up to 4.4 % of their length before breaking. The slope of the stress-strain curves indicate an elastic modulus between 210-550 MPa and the tensile strength (point of fracture) was determined to be 8.0-22 MPa**.** This tensile strength is slightly less than that for polyethylene (20-45 MPa).[8]

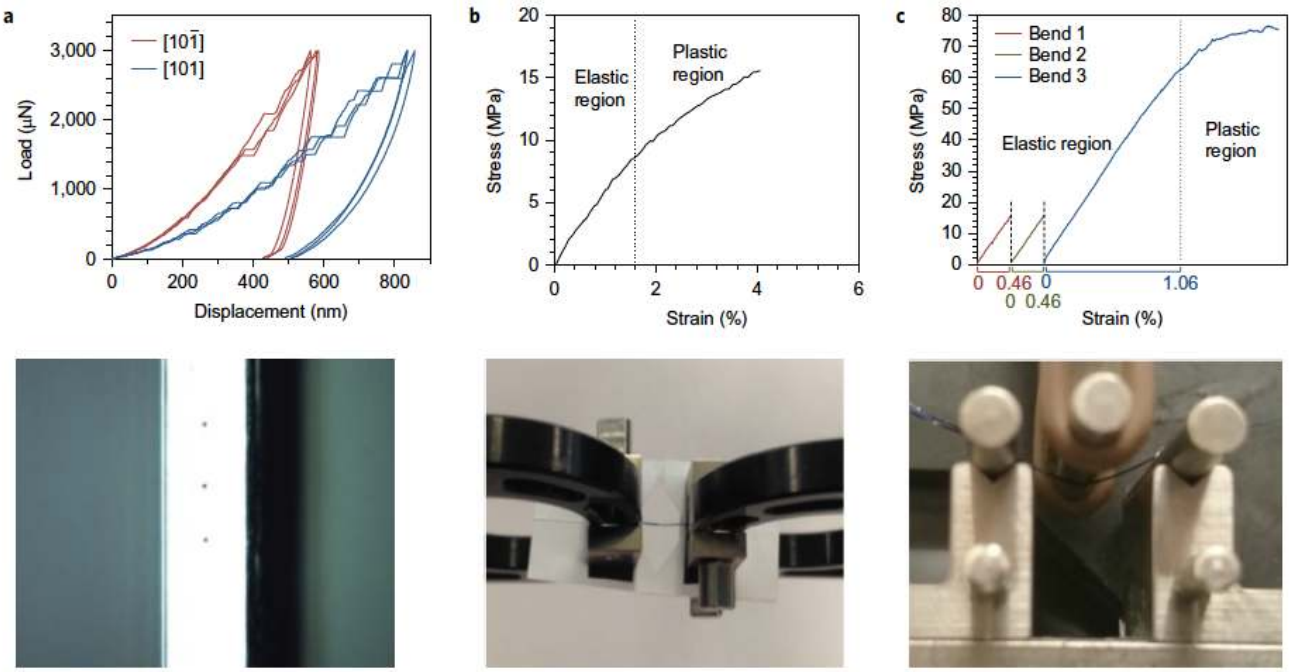

Figure 2 Mechanical properties of single crystals of [Cu(acac)$_2$]. a, Nanoindentation tests performed on (10$\bar{1}$) and (101) faces of [Cu(acac)$_2$] crystals showing anisotropic mechanical properties (top) and picture of a crystal with the three imprints from the indenter after measurement (bottom). **b**, Tensile stress-strain curve of [Cu(acac)$_2$] (top) and picture of a crystal during a tensile test (bottom). **c**, Flexural stress-strain curve of [Cu(acac)$_2$] (top) and picture of a crystal in a 3-point bending test (bottom). The reversibility of the elastic region was proven by bending and unbending a crystal, twice in the elastic region before continuing the test until plastic deformation commenced.

The crystals were then subjected to flexural contortion (*i.e.* bending) *via* 3-point bend tests (Figs. 2c and 2f). To demonstrate the elastic flexibility of the material, a crystal was bent twice with a stress of 15 MPa (giving an elastic modulus of 8 GPa) and then the strain released (Fig. 2f). The crystal was then bent a third time and the strain was increased until plastic deformation commenced (60 MPa). In total, six other crystals were also subjected to flexural stress-strain measurements and the results were similar (see Supplementary Information Section 4). Once again, the clear (initial) linear relationship between stress and strain indicates elastic flexibility with flexure modulus in the range 2-8 GPa. This is comparable to the elasticity observed in soft materials, such as nylon (2-5 GPa).[8]

Microfocus X-ray Diffraction

In order to determine the structural mechanism that permits this remarkable flexibility, microfocus synchrotron X-ray diffraction was employed. A crystal was bent into a loop, mounted on the diffractometer and oriented such that the X-ray beam trajectory was perpendicular to the plane of the loop of the crystal (Fig. 3b). An incremental line map was recorded across the crystals from the outside to the inside of the loop at *ca.* 5 micron intervals. At each interval 20 diffraction images were recorded allowing the determination of the crystal structure at that position in the crystal. A movie illustrating the data acquisition method is provided in the supplementary information (Supplementary Video 2) which shows the trajectory of the line map and the median diffraction image collected at each interval. No phase change was observed throughout the linear map. These mapping experiments demonstrate that the [010] axis of the crystal is significantly elongated (1.5 %) on the outside of the bent crystal and significantly compressed on the inside of the bent crystal (1.9 %). The opposite relationship was observed for the crystal dimensions orthogonal to the length of the crystal. The [101] direction becomes 1.3 % shorter on the outside of the loop and expands on the inside section of the loop (1.7 %). Similarly, although with much less magnitude, there is contraction in the [10$\bar{1}$] direction (0.3 % shorter) on the outside of the loop and expansion (up to 0.4 % longer) on the inside of the loop. Overall, the total variation of length from the inside to the outside of the loop in these different directions is 3.4 % [010], 3.0 % [101] and 0.7 % [10$\bar{1}$]. The deformation is not isotropic. Most of the crystal deformation occurs along the [010] and [101]

directions (*i.e.* in the $(10\bar{1})$ plane) while deformation occurs to a smaller extent along $[10\bar{1}]$. This result is consistent with the nanoindentation measurements by which the (101) face was confirmed to be mechanically softer and more elastic than the $(10\bar{1})$ face. Notably there is almost no change to the overall volume of the unit cell on the inside of the loop compared to the outside (<0.2 %). The density of crystal packing also therefore remains essentially unchanged by bending (Fig. 3c).

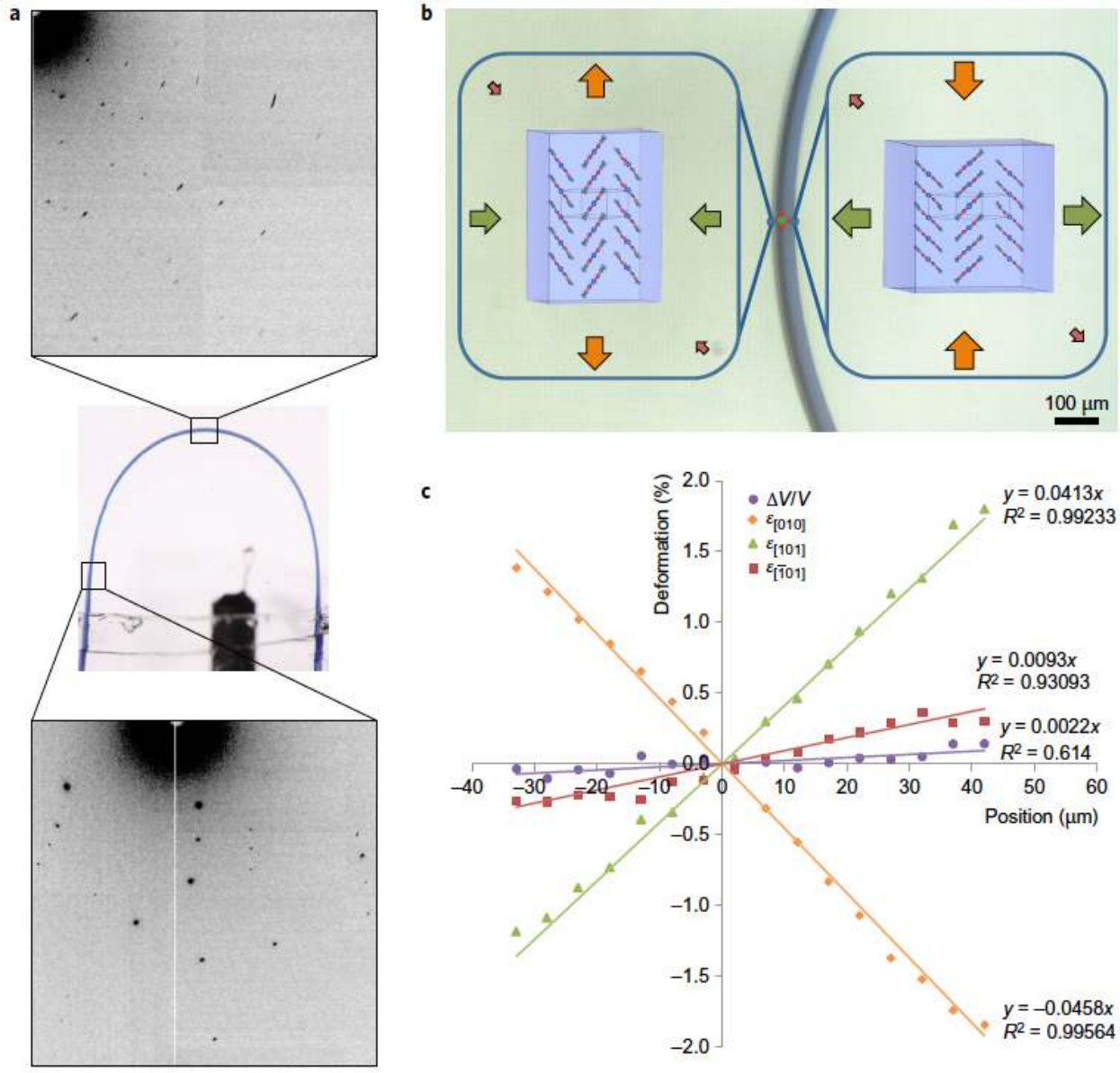

Figure 3 Structure changes in [Cu(acac)$_2$] crystals during flexure. a, A crystal of [Cu(acac)$_2$] bent into a loop and diffraction patterns obtained with a wide (100 µm) beam from both a straight part of the crystal and from a bent part of the crystal. The Bragg peaks from the bent part are significantly broadened. **b**, A bent crystal as mounted at the Australian synchrotron MX2 beamline and view of the structural deformation on the elongated (left) and compressed (right) areas of the crystal. Arrows indicate dimension changes of crystal in the [010] (orange), [101] (green) and $[\bar{1}01]$ (red) directions. **c**, Deformation along natural crystal directions and volume variation from the outside (left) to the inside (right) of a bent crystal determined with a 7.5 µm beam.

Mechanism of Elastic Flexure

Changes in position of the molecules within the crystal lattice with bending were then examined. While the individual molecules of [Cu(acac)$_2$] were found to be identical throughout the sample, the refined crystal structures at each position in the bent crystal show significant differences in arrangement of the molecules with respect to each other. The mean planes of the molecules are approximately orthogonal to the $(10\bar{1})$ plane and the molecules rotate towards planarity with the (010) face as a function of

compression (inside of loop); rotation in the opposite direction occurs with elongation (outside of loop). Importantly though, the distances between the planar [Cu(acac)$_2$] molecules do not change (Supplementary Figs. 22 to 24) rather the molecules rotate in response to the mechanical stress. This rotation of the molecules facilitates the compression in the [010] direction as well as simultaneous expansion in the [101] and [10$\bar{1}$] directions. We have compiled the structures from the outside of the loop and the inside of the loop into an animation (Supplementary Video 2) that demonstrates the change in orientation of the molecules that occurs from the outside of the loop to the inside along with the changes to the unit cell shape to provide a visual representation of the supramolecular mechanism that facilitates elastic bending in these crystals. During elastic bending and/or stretching the local molecular rearrangements required are very small but when added together for the vast numbers of molecules in a single crystal they facilitate significant levels of elastic contortion.

The ability of crystals to bend flexibly has wide-ranging implications. For example, due to the loss of translational symmetry a crystal that is bent (or twisted) is no longer strictly a crystal in the sense that it has lost its long-range order.[15,28] Instead, the "unit cells" of the bent crystal are related by movement along an arc rather than by regular translation. Furthermore, the changes in orientation of molecules within different parts of the bent crystal also *must* influence the physical properties of the crystal. The broadening of Bragg peaks observed for bent crystals of [Cu(acac)$_2$] (Fig. 3a) illustrates this point. In this case, bending the crystal results in a loss of centrosymmetry on the macro-scale, while it is approximately maintained locally, which may enable temporary and reversible second order non-linear optical properties. Similarly, the application of mechanical force to a magnetic material could lead to spin-state switching and the associated magnetic and optical changes.

It has recently been postulated that for a molecular crystal to bend, two criteria must be met. Firstly, the molecules must be connected isotropically by relatively "weak and dispersive" intermolecular interactions and secondly that there must be corrugated crystal packing in which the molecules are interlocked to prevent slippage and consequential plastic deformation.[29-31] Our results show that this is not correct. The intermolecular interactions in [Cu(acac)$_2$] crystals are anisotropic with relatively strong π-stacking in one dimension and only dispersive interactions in the others. Furthermore the molecules are not interlocked. Instead, our results indicate more generally that for elastic bending to occur the molecules must be able to reversibly reorganise to allow compression of the crystal along the interior of the arc with subsequent expansion in orthogonal directions (and vice versa along the exterior of the arc). In [Cu(acac)$_2$] the relatively large area of π-electron density allows sufficient reorientation (rotation) of the molecules without breaking the overall continuity of the crystal packing. In contrast, in molecular crystals that display plastic deformation it is more energetically favourable for certain planes of molecules in the crystal to slip past each other when subjected to strain than it is for the distances between planes to expand or contract.[11,12,29-31] In [Cu(acac)$_2$] we observe no evidence of plastic deformation below 1% strain, but infer a similar mechanism of slippage will be responsible for the plastic deformation that occurs at higher strain values.

The simple mechanism of flexing in [Cu(acac)$_2$] suggests that elastic flexibility will be evident in a much wider array of molecular crystalline materials than previously anticipated. Accordingly, we postulated that it may be possible to further control the mechanical properties of crystals by tuning the strength and type of supramolecular interactions present between molecular materials of this type. Indeed, preliminary investigations into subtly modified crystals (i.e. those that are chemically similar to [Cu(acac)$_2$]) such as *bis*(3-bromo-2,4-pentanedione)copper(II), *bis*(3-chloro-2,4-pentanedione)copper(II), *bis*(benzoylacetonato)copper(II), *bis*(acetylacetonato)palladium(II) and *bis*(3-chloro-2,4-pentanedione)palladium(II) also reveal remarkable elastic flexibility (Supplementary Figs. 25 to 29).

Conclusion

We have reported an elastically flexible metal-organic crystal and determined the mechanism of flexibility with atomic precision. In addition to fundamental interest that surrounds the crystalline state,

stimuli responsive materials like this could enable the design of a range of new hybrid materials that fall between the boundaries of what have typically been regarded as the limitations of hard and soft matter.

Methods

Synthesis of *bis*(acetylacetonato)copper(II) The complex was prepared from acetylacetone and copper(II) nitrate hemi(pentahydrate) following the method of Holtzclaw and Collman.[32] Blue acicular crystals were grown by dissolving the complex in chloroform and allowing the solvent to evaporate slowly. *Elemental Analysis* Found: C, 45.80; H, 5.39%. Calc. for $C_{10}H_{14}O_4Cu$: C, 45.88; H, 5.39%.

Nanoindentation Nanoindendation measurements were performed using a Hysitron TI 950 TriboIndenter system[33] with a Berkovich indenter (three-sided pyramidal indenter with tip radius approximately 100nm, 142.3 ° total included angles). Indention was performed under the load-control setting with a 10s loading period and a 10s unloading period. Flat areas on a crystal's surface suitable for indentation were identified by the on-board optical microscope. To determine truly representative values for the elastic (Young) modulus and hardness the indentation was repeated on a number of sites on a single crystal, and several crystals were tested in the same way for each face. Further details are given in the Supplementary Information.

Tensile stress Tensile stress was measured using a Tytron 250 Microforce Testing System with a displacement resolution of 0.1 μm and a load resolution of 1 μN. The tests were conducted in displacement controlled mode at a rate of 5 mm/min. The samples were fixed with the 250-N Mechanical Clamp Grip and double-sided tape was placed between the grips and the sample to minimise slippage during testing. During the mechanical testing, load (F) and displacement (d) were recorded in real time. Further details are given in the Supplementary Information.

3-Point Bend Tests Three-point bend tests were conducted at room temperature using an Instron Model 5543 universal testing machine with a capacity of 5-N load cell and 3-point bending apparatus with a 15 mm span. A crosshead speed of 2 mm/min was adopted. The individual and average results for six [$Cu(acac)_2$] crystals were determined. Further details are given in the Supplementary Information.

Synchrotron X-ray Studies Synchrotron crystal structures were recorded at the Australian Synchrotron MX beamlines. All measurements were performed at 100(2) K and with the wavelength: $\lambda = 0.7108$ Å. A full data collection was performed at the MX1 beamline with a beam cross-section (at full width at half maximum, FWHM) of 120 by 120 μm. Mapping studies were performed at the MX2 beamline using a micro-collimator producing a beam cross-section of 7.5 by 11.25 μm (FWHM). Data acquisition was performed using Blu-Ice.[34] Data integration and reduction was performed using the XDS package[35]. Using the Olex2 graphical interface[36] the structures were solved with ShelXT[37] and refined with ShelXL.[38]

Data availability The authors declare that the data supporting the findings of this study are available within the Article and its Supplementary Information files, or from the corresponding authors on reasonable request. The X-ray crystal structure data are available free of charge from the Cambridge Crystallographic Data Centre under reference numbers CCDC-1529008-1529042. CCDC-1529008 contains the crystal structure of unbent [$Cu(acac)_2$] at 100(2) K. CCDC-1529009-152924 contain the results of mapping studies on Crystal 1 (structures a-p). CCDC1529025-1529042 contain the results of the mapping studies on Crystal 2 (structures a-r). Full experimental details and crystallographic analysis are given in the Supplementary Information.

REFERENCES

1 Dove, M. T. *Structure and Dynamics: An Atomic View of Materials*. 1st edn, (Oxford University Press,Oxford, 2003).

2 Chen, W., Qi, D.-C., Huang, H., Gao, X. & Wee, A. T. S. Organic–Organic Heterojunction Interfaces: Effect of Molecular Orientation. *Adv. Funct. Mater.* **21**, 410-424 (2011).

3 Shaw, P. E., Wolfer, P., Langley, B., Burn, P. L. & Meredith, P. Impact of Acceptor Crystallinity on the Photophysics of Nonfullerene Blends for Organic Solar Cells. *J. Phys. Chem. C* **118**, 13460-13466 (2014).

4 Huang, M. H. *et al.* Room-Temperature Ultraviolet Nanowire Nanolasers. *Science* **292**, 1897-1899 (2001).

5 Krause, S. *et al.* A pressure-amplifying framework material with negative gas adsorption transitions. *Nature* **532**, 348-352 (2016).

6 Schmidt-Mende, L. *et al.* Self-Organized Discotic Liquid Crystals for High-Efficiency Organic Photovoltaics. *Science* **293**, 1119-1122 (2001).

7 Bronstein, H. *et al.* Thieno[3,2-b]thiophene−Diketopyrrolopyrrole-Containing Polymers for High-Performance Organic Field-Effect Transistors and Organic Photovoltaic Devices. *J. Am. Chem. Soc.* **133**, 3272-3275 (2011).

8 Somiya, S. (ed). *Handbook of Advanced Ceramics: Materials, Applications, Processing, and Properties*. 2nd edn, (Academic Press,Oxford, 2013).

9 Reddy, C. M., Rama Krishna, G. & Ghosh, S. Mechanical properties of molecular crystals-applications to crystal engineering. *CrystEngComm* **12**, 2296-2314 (2010).

10 Reddy, C. M., Padmanabhan, K. A. & Desiraju, G. R. Structure-Property Correlations in Bending and Brittle Organic Crystals. *Cryst. Growth Des.* **6**, 2720-2731 (2006).

11 Panda, M. K. *et al.* Spatially resolved analysis of short-range structure perturbations in a plastically bent molecular crystal. *Nat. Chem.* **7**, 65-72 (2015).

12 Reddy, C. M. *et al.* Structural basis for bending of organic crystals. *Chem. Commun.*, 3945-3947 (2005).

13 Duyker, S. G., Peterson, V. K., Kearley, G. J., Studer, A. J. & Kepert, C. J. Extreme compressibility in LnFe(CN)6 coordination framework materials via molecular gears and torsion springs. *Nat. Chem.* **8**, 270-275 (2016).

14 Goodwin, A. L. *et al.* Colossal Positive and Negative Thermal Expansion in the Framework Material $Ag_3[Co(CN)_6]$. *Science* **319**, 794-797 (2008).

15 Commins, P., Desta, I. T., Karothu, D. P., Panda, M. K. & Naumov, P. Crystals on the move: mechanical effects in dynamic solids. *Chem. Commun.* **52**, 13941-13954 (2016).

16 Takamizawa, S. & Miyamoto, Y. Superelastic Organic Crystals. *Angew. Chem., Int. Ed.* **53**, 6970-6973 (2014).

17 Werner, A. Über Acetylacetonverbindungen des Platins. *Ber. Deut. Chem. Ges.* **34**, 2584-2593 d (1901).

18 Starikova, Z. A. & Shugam, E. A. Crystal chemical data for inner complexes of β-diketones. *J. Struct. Chem.* **10**, 267-269 (1969).

19 Lebrun, P. C., Lyon, W. D. & Kuska, H. A. Crystal structure of bis(2,4-pentanedionato)copper(II). *J. Crystallogr. Spectrosc. Res.* **16**, 889-893 (1986).

20 Vreshch, V. D., Yang, J.-H., Zhang, H., Filatov, A. S. & Dikarev, E. V. Monomeric Square-Planar Cobalt(II) Acetylacetonate: Mystery or Mistake? *Inorg. Chem.* **49**, 8430-8434 (2010).

21 Golchoubian, H. Redetermination of Crystal Structure of Bis(2,4-pentanedionato)copper(II). *Asian J. Chem.* **20**, 5834-5838 (2008).

22 Hamid, M., Mazhar, M., Zeller, M. & Hunter, A. D. CCDC 281026. *CSD Communication*, doi:DOI: 10.5517/cc9ffch (2005).

23 Berry, G., Callon, G., Gowans, B., Low, J. N. & Smith, R. CCDC 228882. *CSD Communication*, doi: DOI: 10.5517/cc7p59c (2004).

24 Janiak, C. A critical account of π-π stacking in metal complexes with aromatic nitrogen containing ligands. *J. Chem. Soc., Dalton Trans.*, 3885-3896 (2000).
25 Hunter, C. A. & Sanders, J. K. M. The Nature of π-π Interactions. *J. Am. Chem. Soc.* **112**, 5525-5534 (1990).
26 Heine, K. B. *et al.* Complexation, Computational, Magnetic, and Structural Studies of the Maillard Reaction Product Isomaltol Including Investigation of an Uncommon π Interaction with Copper(II). *Inorg. Chem.* **50**, 1498-1505 (2011).
27 Tan, J. C. & Cheetham, A. K. Mechanical properties of hybrid inorganic-organic framework materials: establishing fundamental structure-property relationships. *Chemical Society Reviews* **40**, 1059-1080 (2010).
28 Keen, D. A. & Goodwin, A. L. The crystallography of correlated disorder. *Nature* **521**, 303-309 (2015).
29 Ghosh, S. & Reddy, C. M. Elastic and Bendable Caffeine Cocrystals: Implications for the Design of Flexible Organic Materials. *Angew. Chem., Int. Ed.* **51**, 10319-10323 (2012).
30 Ghosh, S., Mishra, M. K., Ganguly, S. & Desiraju, G. R. Dual Stress and Thermally Driven Mechanical Properties of the Same Organic Crystal: 2,6-Dichlorobenzylidene-4-fluoro-3-nitroaniline. *J. Am. Chem. Soc.* **137**, 9912-9921 (2015).
31 Ghosh, S., Mishra, M. K., Kadambi, S. B., Ramamurty, U. & Desiraju, G. R. Designing Elastic Organic Crystals: Highly Flexible Polyhalogenated N-Benzylideneanilines. *Angew. Chem., Int. Ed.* **54**, 2674-2678 (2015).
32 Holtzclaw, H. F., Johnson, K. W. R. & Hengeveld, F. W. Polarographic Reduction of the Copper Derivatives of Several 1,3-Diketones in Various Solvents. *J. Am. Chem. Soc.* **74**, 3776-3778 (1952).
33 *TI 950 TriboIndenter User Manual*. Revision 9.2.1211 edn, (Hysitron Incorporated,Minneapolis, MN, 2011).
34 McPhillips, T. M. *et al.* Blu-Ice and the Distributed Control System: software for data acquisition and instrument control at macromolecular crystallography beamlines. *J. Synchrotron Rad.* 9, 401-406 (2002).
35 Kabsch, W. Automatic processing of rotation diffraction data from crystals of initially unknown symmetry and cell constants. *J. Appl. Cryst.* **26**, 795-800 (1993).
36 Dolomanov, O. V., Bourhis, L. J., Gildea, R. J., Howard, J. A. K. & Puschmann, H. OLEX2: a complete structure solution, refinement and analysis program. *J. Appl. Cryst.* **42**, 339-341 (2009).
37 Sheldrick, G. M. SHELXT - Integrated space-group and crystal-structure determination. *Acta Cryst.* **A71**, 3-8 (2015).
38 Sheldrick, G. M. Crystal structure refinement with SHELXL. *Acta Cryst.* **C71**, 3-8 (2015).

Supplementary Information is available in the online version of the paper.

Acknowledgements We thank the Australian Research Council for support. Part of this research was undertaken on the MX1 and MX2 beamlines of the Australian Synchrotron, Clayton, Victoria, Australia. We thank the Australian Synchrotron for travel support and their staff for assistance. We thank the Central Analytical Research Facility, Queensland University of Technology and the University of Queensland for support.

Author Contributions A.W., M.C.P. and A.G. synthesised the materials investigated. A.G., A.W., M.C.P., J.K.C. and J.C.M. performed X-ray measurements. A.W., A.G., M.C.P., Y.X., C.Y. and G.E. performed mechanical measurements. J.K.C and J.C.M conceptualised the studies and directed the research. A.W., A.G., M.C.P., J.K.C. and J.C.M. wrote the manuscript.

Author Information Reprints and permissions information is available at www.nature.com/reprints. The authors declare no competing financial interests. Readers are welcome to comment on the online version of the paper. Correspondence and requests for materials should be addressed to J. K. Clegg

(j.clegg@uq.edu.au) or J. C. McMurtrie (j.mcmurtrie@qut.edu.au).

FIGURE CAPTIONS

Figure 1 Crystal Structure of [Cu(acac)$_2$]. a, Chemical structure of [Cu(acac)$_2$]. **b**, A [Cu(acac)$_2$] crystal tied (reversibly) in an overhand knot. **c**, Two views of the crystal structure of unbent [Cu(acac)$_2$] viewed along the [010] and [10$\bar{1}$] directions as determined by face indexing.

Figure 2 Mechanical properties of single crystals of [Cu(acac)$_2$]. a, Nanoindentation tests performed on (10$\bar{1}$) and (101) faces of [Cu(acac)$_2$] crystals showing anisotropic mechanical properties (top) and picture of a crystal with the three imprints from the indenter after measurement (bottom). **b**, Tensile stress-strain curve of [Cu(acac)$_2$] (top) and picture of a crystal during a tensile test (bottom). **c**, Flexural stress-strain curve of [Cu(acac)$_2$] (top) and picture of a crystal in a 3-point bending test (bottom). The reversibility of the elastic region was proven by bending and unbending a crystal, twice in the elastic region before continuing the test until plastic deformation commenced.

Figure 3 Structure changes in [Cu(acac)$_2$] crystals during flexure. a, A crystal of [Cu(acac)$_2$] bent into a loop and diffraction patterns obtained with a wide (100 μm) beam from both a straight part of the crystal and from a bent part of the crystal. The Bragg peaks from the bent part are significantly broadened. **b**, A bent crystal as mounted at the Australian synchrotron MX2 beamline and view of the structural deformation on the elongated (left) and compressed (right) areas of the crystal. Arrows indicate dimension changes of crystal in the [010] (orange), [101] (green) and [$\bar{1}$01] (red) directions. **c**, Deformation along natural crystal directions and volume variation from the outside (left) to the inside (right) of a bent crystal determined with a 7.5 μm beam.